

磁控溅射铱薄膜的表面形态与取向演变的控制优化

夏天，黄珂，郑宇亭，陈良贤，刘金龙，魏俊俊，李成明

(北京科技大学 新材料技术研究院, 北京 100083)

摘要：目的 研究磁控溅射制备金属 Ir 膜的过程中溅射参数对 Ir 膜表面微结构和晶体质量的影响，制备高质量(100)取向的外延 Ir 膜，为单晶金刚石的异质外延生长奠定重要基础。**方法** 通过磁控溅射技术在单一改变参数(溅射功率、溅射厚度)的条件下制备金属 Ir 膜，通过分析原子力显微镜、扫描电子显微镜、X 射线衍射、电子背散射衍射等测试结果，研究了各条件对所制备 Ir 膜粗糙度、表面形貌、晶体结构和取向的影响，并通过摇摆曲线衡量真空退火对薄膜晶体质量的优化效果。**结果** 在(100)MgO 衬底上外延生长的 Ir 膜具有均匀的微结构，该结构由规则且紧密的矩形颗粒排列而成。薄膜表面微结构特征尺寸随溅射功率升高而逐渐减小；当功率为 45 W 时，Ir(200)X 射线衍射峰强度最大、半高宽最宽；而随着厚度的增大，Ir(200)X 射线衍射峰的半高宽及强度均增大。经优化的 Ir 膜表面光滑($R_a < 0.5 \text{ nm}$)、薄膜晶体质量高($\theta_{FWHM} < 0.5^\circ$)。**结论** 功率、厚度和退火处理都会影响薄膜晶体质量和表面微结构尺寸，合适的功率和厚度结合退火处理能获得具有特定表面微结构的高质量 Ir 膜。

关键词：磁控溅射；功率；厚度；Ir 膜；表面微结构；晶体质量

中图分类号：TG174.442 **文献标识码：**A **文章编号：**1001-3660(2023)03-0338-07

DOI：10.16490/j.cnki.issn.1001-3660.2023.03.031

Control and Optimization of Surface Morphology and Orientation Evolution of Iridium Films Prepared by Magnetron Sputtering

XIA Tian, HAUNG Ke, ZHENG Yu-ting, CHEN Liang-xian, LIU Jin-long, WEI Jun-jun, LI Cheng-ming

(Institute of Advanced Materials Technology, University of Science and Technology Beijing, Beijing 100083, China)

ABSTRACT: The preparation of high-quality Iridium films is an important step in the heteroepitaxy growth of single crystal diamond, it is self-evident that the irreplaceable role of Ir films in this area. To establish a solid foundation for the heteroepitaxy growth of single crystal diamond and prepare high quality (100) oriented Ir films, it is necessary to figure out the influence of sputtering parameters and annealing process on the quality of Ir films. The preparation of Ir films was based on RF magnetron

收稿日期：2022-02-23；修订日期：2022-05-29

Received: 2022-02-23; **Revised:** 2022-05-29

基金项目：国家自然科学基金(11291211); 北京市自然科学基金(08910109)

Fund: National Natural Science Foundation of China(11291211); Beijing Natural Science Foundation(08910109)

作者简介：夏天(1996—)，男，硕士研究生，主要研究方向为金刚石膜科学与技术。

Biography: XIA Tian(1996-), Male, Postgraduate, Research focus: diamond film science and technology.

通讯作者：李成明(1962—)，男，博士，教授，主要研究方向为薄膜科学与技术。

Corresponding author: LI Cheng-ming(1962-), Male, Doctor, Professor, Research focus: film science and technology.

引文格式：夏天，黄珂，郑宇亭，等. 磁控溅射铱薄膜的表面形态与取向演变的控制优化[J]. 表面技术, 2023, 52(3): 338-344.

XIA Tian, HAUNG Ke, ZHENG Yu-ting, et al. Control and Optimization of Surface Morphology and Orientation Evolution of Iridium Films Prepared by Magnetron Sputtering[J]. Surface Technology, 2023, 52(3): 338-344.

sputtering, and single crystal (100) MgO with high crystal quality ($\theta_{FWHM}=0.045^\circ$) and smooth surface ($Ra=0.016\text{ nm}$) was used as substrate. This research was carried out as a single factor (power and thickness) experiment, when the power was studied, the range was set as 25 W, 45 W, 65 W, 85 W and 105 W, and when the thickness was studied, the range was set as 36 min, 48 min, 60 min, 72 min and 84 min, corresponding to the Ir films thickness of 150 nm, 200 nm, 250 nm, 300 nm and 350 nm, respectively. And the samples were characterized by atomic force microscopy, scanning electron microscopy, X-ray diffraction and electron back scattering diffraction, the influence of parameters on roughness, surface morphology, crystal structure and orientation was analyzed. The annealing experiment was based on vacuum annealing furnace, this experiment was carried out as a before-after experiment in the same sample. The Ir films 200 nm and 350 nm thick were used as blank space group in this experiment, and the films were set as experimental group after the characterization step. And then the Ir films of experimental group were adopted vacuum annealing treatment at 950 °C for 1 h. The effect of vacuum annealing treatment on the crystal quality of Ir films was analyzed by rocking curve. The Ir films grown on (100) MgO substrate had a uniform microstructure, which was composed of regular and closely arranged rectangular particles. As the power increased, the characteristic size of microstructure on the surface of Ir films gradually decreased. The films with narrowest FWHM and strongest Ir(200) peak were obtained at 45 W, too high or too low power would degrade the crystalline quality of the Ir films; the FWHM and intensity of Ir films increased with the increase of thickness, the main reason for this phenomenon was the enhanced crystallinity of the Ir films, although the upper Ir films shielding substrate signals also contributed, but this part was eliminated by normalization of XRD patterns, the effect of Ir films thickness on the roughness and grain size was very limited. After annealing process, as was shown in the rocking curve patterns, the Ir(200) peak strength of rocking curve was enhanced and the FWHM was reduced, the crystal quality is obviously optimized. Eventually the high quality ($\theta_{FWHM}<0.5^\circ$) Ir films obtain smooth surface ($Ra<0.5\text{ nm}$) and highly preferred orientation. Power、thickness and annealing treatment can affect crystal quality and the size of microstructure. High quality Ir films with specific surface microstructure can be obtained by appropriate power and thickness combined with annealing treatment.

KEY WORDS: magnetron sputtering; power; thickness; Ir films; surface microstructure; crystal quality

金属铱(Ir)具有高熔点、耐腐蚀、高强度、高电导率等优异的理化性质, 因而在诸多高新技术领域起到了不可替代的作用^[1-3]。特别地, 当碳在铱中的溶解度超限^[4]将会有大量的碳被排斥到Ir表面, 为形核过程提供碳源和形核位点, 该溶解-析出过程促使金刚石晶粒迁移、旋转并达到一致取向。Verstraete等^[4]通过计算研究多种衬底与金刚石间的相互作用, 也证明了Ir是外延金刚石最合适的选择。诸多科研成果表明, 金属Ir在金刚石异质外延领域发挥的作用无可替代, 但这同时也对金属Ir膜结构与性能的要求更为严苛, 尽管有极个别专利^[5]采用Ir金属片作为衬底材料, 可单晶Ir薄片制造难度大、生产成本高, 导致高质量Ir膜的制备和应用难以继。

为解决上述问题, 在异质衬底表面进行Ir膜的外延生长成了一种行之有效的方案, 如何在特定单晶衬底上制备高质量、大尺寸的Ir过渡层成了外延单晶金刚石的决定性因素^[6-7]。有众多科研人员在Ir膜的异质外延生长领域展开了大量研究^[8-10], 这些研究大多基于MgO^[11]、Al₂O₃^[9]、Si/YSZ^[13]、Si/SrTiO₃^[14]等衬底展开, 其中围绕MgO(100)单晶外延Ir膜的研究历史最为久远, 众多研究中不乏基于(100)Ir/(100)MgO衬底成功异质外延单晶金刚石^[15-17]的成果。早在1996年Ohtsuka等^[18]就在单晶MgO(100)

剥离面上采用离子枪溅射获得500 nm厚度的Ir层, 此后基于MgO(100)衬底外延的Ir膜质量越来越高, 还开发出图案化生长法外延金刚石^[19-20]。当然研究人员也不会错过当下广泛应用的传统半导体材料Si, 但Ir-Si间会形成的多种低熔点非立方相的化合物, 阻碍了直接外延。Stritzker等^[21]通过在Si上沉积YSZ层, 再利用电子束蒸发法在YSZ上获得了高质量Ir膜, 也有少量研究在Si上制备CaF₂过渡层, 并基于Si/CaF₂衬底制备了不同取向的Ir层^[22]。Dai等^[23]利用电子束蒸发法在(11-20)蓝宝石衬底上制备了Ir膜。Vargas等^[24]的研究表明, 通过MOCVD在(11-20)Al₂O₃上制备的Ir膜取向为(200), 而在(11-20)Al₂O₃和(0001)Al₂O₃衬底上却是(111)取向。Khoa等^[25]基于Si/YSZ衬底制备的Ir膜, 其取向与沉积速度有关:当沉积速度低至0.03 μm/h时, 获得的Ir膜为(100)高择优取向, 当速度加快则呈现出(111)高择优取向。后来Sell等^[26]以0.004 nm/s的速率沉积前20 nm, 然后使用0.05 nm/s的速率沉积180 nm的Ir膜, 制备了摇摆曲线半高宽仅为0.18°的高质量Ir膜。

金属Ir膜晶体质量和表面微结构对单晶金刚石异质外延的形核有重要影响。因此, 磁控溅射获取Ir膜的系统研究对于控制Ir膜表面微结构尺寸、优化金属Ir膜的晶体质量, 很有意义。本研究主要围绕射频

磁控溅射法展开,研究功率和厚度对Ir膜表面微结构和晶体取向的影响,为金属Ir膜的磁控溅射法制备提供更多的数据支撑。

1 试验

1.1 Ir膜的制备

所用设备为JCP-500M2型磁控溅射镀膜机,以纯度为99.95%的Ir靶(Ir靶尺寸为 $\phi 50.8\text{ mm} \times 5\text{ mm}$)为溅射靶材,以纯度为99.999%的氩气为工作气体。沉积Ir膜前,首先对基片进行偏压轰击以去除基片表面分子级的杂质,所采用的偏压为800V、占空比为50%。随后预溅射5min,以确保稳定的辉光、稳定的溅射速率以及清洁的靶面。沉积温度为500℃,背底真空为 $2 \times 10^{-4}\text{ Pa}$,沉积时腔压为0.64Pa,氩气流量为16mL/min,工作台以30r/min的速度转动。另外,沉积过程中在衬底上施加60V的偏压,以增

加到达MgO基片表面的粒子数量及粒子迁移率。具体溅射功率和沉积时间见表1。

表1 沉积金属Ir膜的工艺参数
Tab.1 Parameters of Ir films deposition

Group	Power/W	Time/min	Group	Power/W	Time/min
a	25	200	f	65	36
b	45	88	g	65	48
c	65	48	h	65	60
d	85	26	i	65	72
e	105	23	j	65	84

基体材料采用(100)取向的单晶MgO基片($10\text{ mm} \times 10\text{ mm} \times 0.5\text{ mm}$),依次采用丙酮、酒精超声清洗,并烘干备用。单晶MgO的粗糙度和摇摆曲线如图1所示,MgO(100)单晶基片表面平坦并具有优异的晶体质量,其粗糙度低至0.016nm,其摇摆曲线半高宽仅为0.0452°。

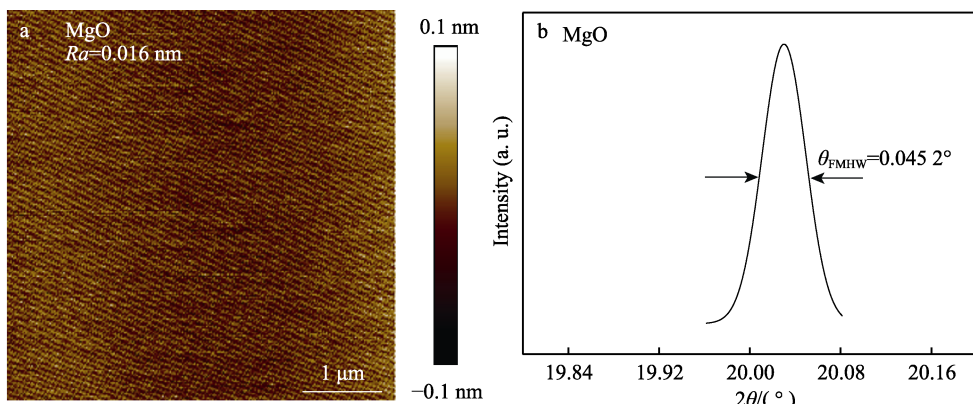


图1 单晶MgO的AFM图像(a)和摇摆曲线(b)
Fig.1 AFM image (a) and rocking curve (b) of single crystal MgO

1.2 Ir膜的测试与表征

采用Bruker Multimode 8型原子力显微镜在 $5\text{ }\mu\text{m} \times 5\text{ }\mu\text{m}$ 采样区域对薄膜粗糙度进行表征,并结合ZEISS GeminiSEM 500型场发射扫描电子显微镜在放大倍数为30 000的条件下对表面形貌进行表征。采用Rigaku SmartLab 9 kW型X射线衍射仪常规theta-2theta联动扫描测试对Ir膜晶体结构进行测试分析,同时通过Rigaku SmartLab S2型X射线衍射仪配套测角仪进行摇摆曲线的测试,联合ZEISS GeminiSEM 350型场发射扫描电子显微镜配套的电子背散射衍射对Ir膜的取向进行表征,以分析Ir膜的晶体质量。

2 结果与讨论

2.1 溅射功率对Ir膜组织的影响

图2、图3分别为不同磁控溅射功率下获得的Ir

膜的表面微结构和XRD谱图。如图2所示,在低功率(25W)下,Ir膜表面网格状结构松散并形成较多明显的凹陷,网格结构尺寸也相对较大,而在高功率(105W)下,Ir膜表面网格状结构细密紧凑,网状结构尺寸也随之减小。如图2和图4所示,溅射功率从25W均匀上升到105W,Ir膜晶粒尺寸从350nm单调下降到150nm。根据图2a—e显示的特征可以看出,较高的粒子能量不仅导致晶粒尺寸快速减小,也导致Ir膜变得更加致密,薄膜黑色处代表的凹陷部分也随之减少。

由于功率的增大会导致轰击薄膜表面的离子密度和能量增大,致使到达衬底的粒子能量增加,所以粒子在抵达衬底表面后,其扩散程度也随之增大。在低功率下粒子能量相对较低,粒子的能量不仅影响薄膜内部组织,同时也影响薄膜的表面微结构尺寸。低能量的粒子在衬底表面扩散不充分,较低的粒子能量导致薄膜表面网格状结构松散并形成较多的明显的凹陷,相对应的Ir膜晶粒尺寸高达350nm。根据Ir膜的AFM图像借助NanoScope Analysis软件计算可

得 Ir 膜的平均粗糙度 R_a , 具体数值如图 2 所示。显然, 尽管低功率下薄膜微观结构松散且存在明显的凹陷, 但在溅射功率为 45 W 时, 薄膜就已经十分致密、凹陷较少, 粗糙度也低至 0.515 nm, 薄膜的粗糙度随着溅射功率的增加呈现逐渐降低的趋势, 但在 45 W 之后, 基本稳定在 0.5 nm 左右。

由图 3 可知, 在温度为 500 ℃下溅射所得样品均有 4 个尖锐的衍射峰: 来自衬底 MgO(200)和 MgO(400)的峰以及 Ir(200)和 Ir(400)的峰, 未观察到其他杂峰, 说明所获得的薄膜组分单一, 且不同条件下获得的薄膜均为高度择优取向的织构, 薄膜质量

高。将各试验条件下 MgO(200)衍射峰处理为同等强度, 其他衍射峰均等比例缩放, 可以看到, Ir(200)衍射峰强度明显高于 Ir(400)衍射峰, 各条件下衍射峰 Ir(200)/Ir(400)强度比值均在 100 左右, Ir 膜呈现出(100)高择优取向, 原因可能是由于衬底是(100)取向, Ir 膜沉积在单晶 MgO 表面时 Ir(100)面与衬底的界面能最低^[12], 所以 Ir 膜始终沿着(100)取向生长。

溅射功率从 25 W 提高到 105 W, 如图 4 所示, 在 45 W 时 Ir 膜(200)衍射峰强度达到最强、半高宽最小, Ir 膜的结晶化程度最高, Ir 膜的衍射峰强度甚至超过了单晶 MgO(100)衬底, 此时 Ir 膜的晶体质量达

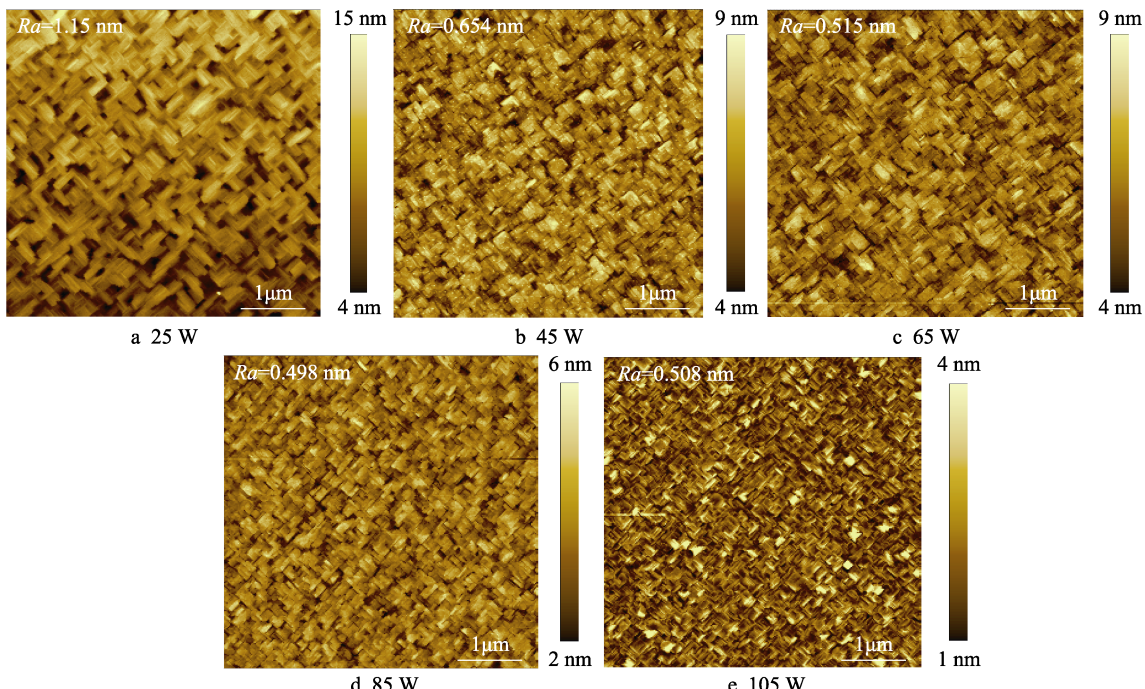


图 2 不同溅射功率沉积的 Ir 膜表面微结构
Fig.2 Surface microstructure of Ir films deposited with different sputtering powers

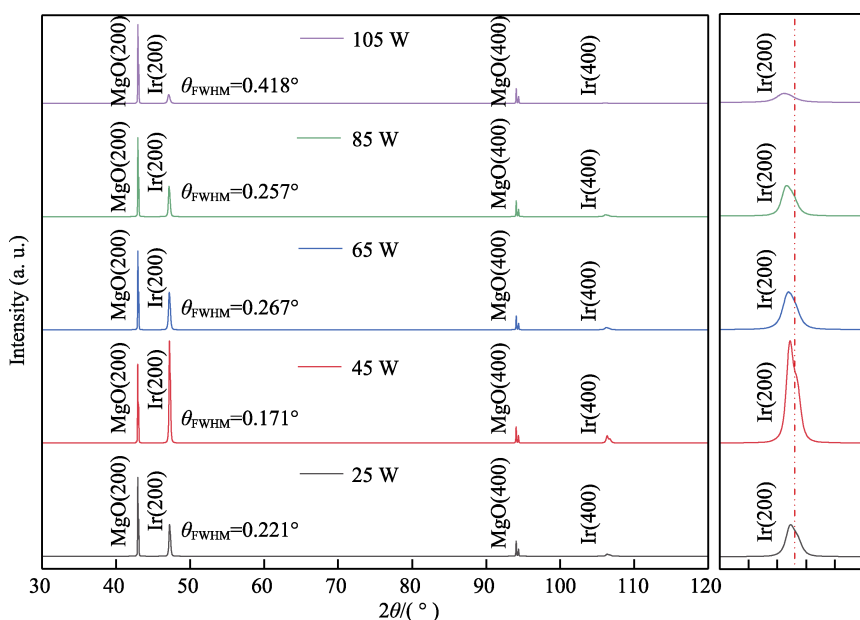


图 3 不同溅射功率下 Ir 膜 XRD 谱图
Fig.3 XRD patterns of Ir films under different sputtering powers

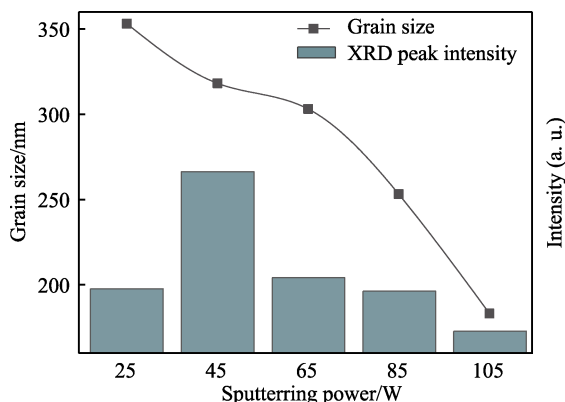


图4 不同溅射功率下晶粒尺寸和XRD衍射峰强度
Fig.4 Grain size and X-ray diffraction peak intensity under different sputtering powers

到最优，呈现出(100)高度择优的取向。这说明在所设置的功率范围内，晶体质量随着功率的降低而提高，但溅射功率过低也对晶体质量有着不利的影响，具体表现在其衍射峰宽度增加、强度降低。

2.2 沉积厚度对Ir膜组织的影响

由图5可知，各功率下精确的Ir膜沉积速率，因此可以通过精确控制溅射时间来实现特定厚度薄膜的获取，并在不同溅射时间下获得厚度分别为150、200、250、300、350 nm的Ir膜。由图6—8可知，Ir膜在厚度为150 nm时已经形成了连续的薄膜，且随着Ir膜厚度的增加，薄膜的晶粒大小和表面粗糙度没有明显变化，晶粒大小均在300~350 nm之间，粗糙度也稳定在0.6 nm左右。

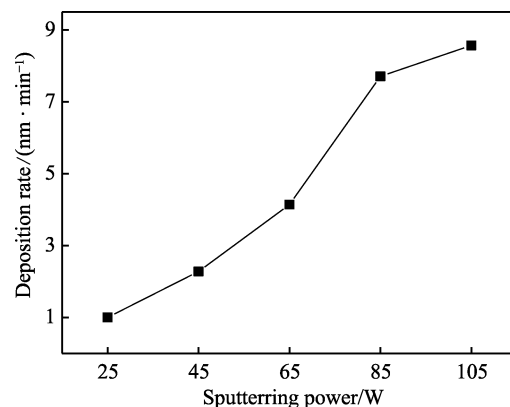


图5 不同溅射功率下Ir膜沉积速率
Fig.5 Ir films deposition rate under different sputtering power

为了深入理解磁控溅射制备金属Ir膜取向生长过程，对不同厚度Ir膜进行了物相结构分析。如图7所示，薄膜越厚衍射峰变强并逐渐宽化，相对于150 nm和200 nm，在250 nm时Ir(200)衍射峰已经十分明显，而且随着厚度的增加，衍射峰强度不断攀升，虽然逐渐增厚的Ir膜会削弱底层MgO的信号，但将各试验条件下MgO(200)衍射峰处理为同等强度，其他衍射峰均等比例缩放后，该部分贡献已经消除。Ir(200)衍射峰的增强更多的是Ir膜的结晶性增强导致的衍射峰强度增大，而Ir(200)衍射峰宽化的可能原因是随着膜厚的增加，来自衬底的模板效应减弱，上层的Ir只能沿着其下层的Ir膜晶格进行排列，Ir薄膜的晶体质量逐渐降低。

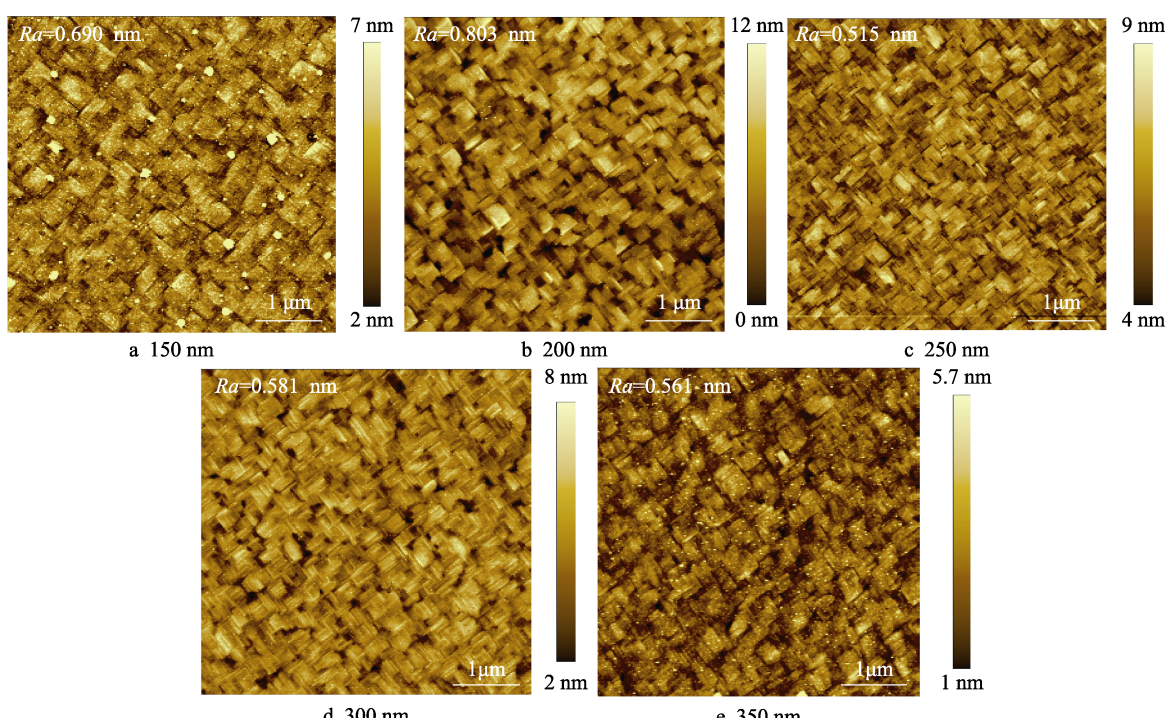


图6 不同厚度Ir膜表面微结构
Fig.6 Surface microstructure of Ir films with different thicknesses

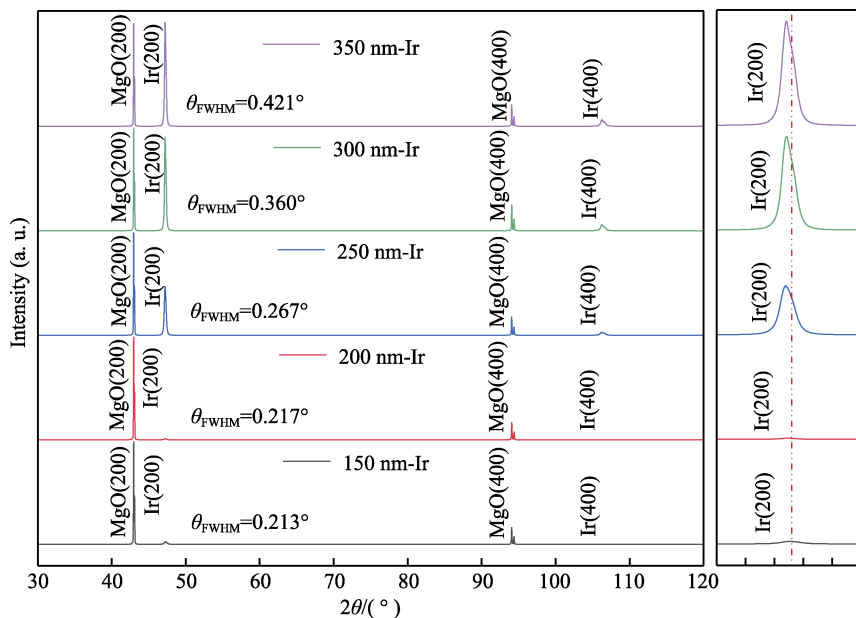


图 7 不同厚度 Ir 膜的 XRD 谱图
Fig.7 XRD patterns of Ir films with different thicknesses

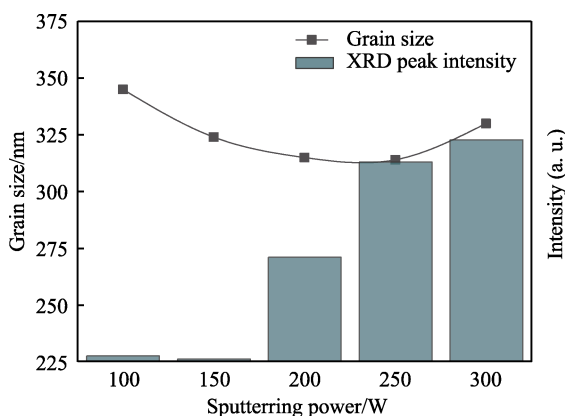


图 8 不同厚度 Ir 膜晶粒尺寸和 XRD 衍射峰强度
Fig.8 Grain size and XRD diffraction peak intensity of Ir films with different thicknesses

2.3 退火处理对 Ir 膜组织的影响

考虑到退火能够有效增强薄膜的结晶化、提高薄膜的晶体质量, 所以为达到进一步优化晶体质量的目的, 选取厚度分别为 200 nm 和 350 nm 的样品在真空度为 2×10^{-4} Pa、温度为 950 °C 条件下进行 1 h 的退火试验。图 9 表明不同厚度的 Ir 膜经过退火过程, Ir (200) 衍射峰半高宽减小并保证了衍射主峰经退火过程仍具有对称性。不同厚度样品经过退火, 其 Ir (200) 衍射峰强度增加、半高宽变小, 表明薄膜结晶性优化、取向增强, 晶体质量得到了一定的提高。

经过以上一系列优化过程, 最终利用磁控溅射法制备了高质量 Ir 膜, 表 1 所列试验条件下的各组样品均获得了具有图 10a 所示网格状结构的 Ir 膜: 薄膜表面呈现出台阶状貌, 表面的晶粒均具有较为均匀的长条形微结构, 由规则且紧密排列的矩形颗粒排列而

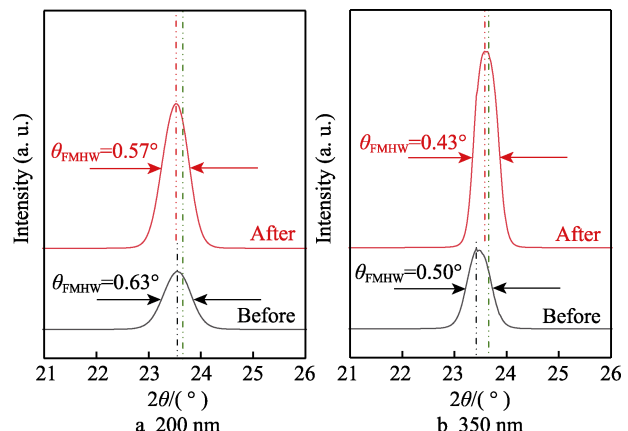


图 9 溅射功率为 65 W 沉积的 200 nm (a) 和 350 nm (b) Ir 膜退火前后摇摆曲线
Fig.9 Rocking curves of 200 nm (a) and 350 nm (b) Ir films deposited at 65 W sputter power before and after annealing

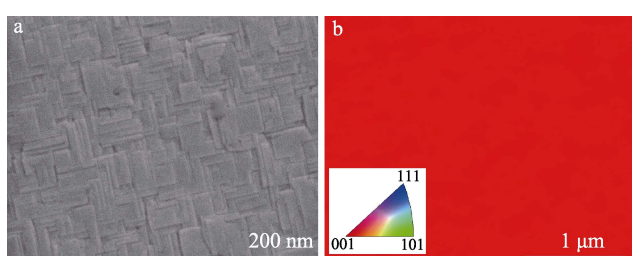


图 10 溅射功率为 65W 沉积 Ir 膜的表面微结构 (a) 及其 EBSD (b)
Fig.10 Surface microstructure (a) and EBSD (b) measurements of Ir films deposited by sputtering power of 65 W

成并布满整个平面。图 10b 为薄膜的 EBSD 取向分布图, 该图全部由纯红色组成, 说明 Ir 膜呈现高度的 (100) 取向分布。

3 结论

通过磁控溅射法在 500 °C/0.64 Pa 条件下制备的 Ir 膜表面具有网格状结构，该结构由规则且紧密排列的矩形颗粒排列成台阶状。通过对不同溅射功率和不同溅射时间下得到的 Ir 膜进行研究，重点表征分析其表面微结构和晶体质量的变化，研究结果显示：在以上所有试样条件下获得的 Ir 膜均具有高择优取向织构的基本特征。Ir 膜表面微结构受溅射功率的影响显著：功率越高，晶粒越细小，表面网格状结构越紧凑，表面凹陷也随之减少；功率越低，晶体质量越高，但溅射功率过低对晶体质量有不利的影响；薄膜厚度与溅射时间直接相关，而薄膜越厚，其结晶性越好，但取向会发生宽化。此外退火能够增强磁控溅射法生长的 Ir 膜结晶性，能够在一定程度上提升 Ir 膜的晶体质量。

参考论文：

- [1] YAMABE-MITARAI Y, GU Y, HUANG C, et al. Platinum-Group-Metal-Based Intermetallics as High-Temperature Structural Materials[J]. *JOM*, 2004, 56(9): 34-39.
- [2] HECKER S S, ROHR D L, STEIN D F. Brittle Fracture in Iridium[J]. *Metallurgical Transactions A*, 1978, 9(4): 481-488.
- [3] AALTONEN T, RITALA M, SAMMELSELG V, et al. Atomic Layer Deposition of Iridium Thin Films[J]. *Journal of the Electrochemical Society*, 2004, 151(8): G489.
- [4] VERSTRAETE M J, CHARLIER J C. Why is Iridium the Best Substrate for Single Crystal Diamond Growth?[J]. *Applied Physics Letters*, 2005, 86(19): 191917.
- [5] NOGUCHI R. Manufacturing Method of Diamond Film: C30B25/10[P]. 2015-12-23.
- [6] SCHRECK M, HÖRMANN F, ROLL H, et al. Diamond Nucleation on Iridium Buffer Layers and Subsequent Textured Growth: A Route for the Realization of Single-Crystal Diamond Films[J]. *Applied Physics Letters*, 2001, 78(2): 192-194.
- [7] FISCHER M, GSELL S, SCHRECK M, et al. Preparation of 4-Inch Ir/YSZ/Si(001) Substrates for the Large-Area Deposition of Single-Crystal Diamond[J]. *Diamond and Related Materials*, 2008, 17(7-10): 1035-1038.
- [8] GALLHEBER B C, KLEIN O, FISCHER M, et al. Propagation of Threading Dislocations in Heteroepitaxial Diamond Films with (111) Orientation and Their Role in the Formation of Intrinsic Stress[J]. *Journal of Applied Physics*, 2017, 121(22): 225301.
- [9] KIM S W, KAWAMATA Y, TAKAYA R, et al. Growth of High-Quality One-Inch Free-Standing Heteroepitaxial (001) Diamond on (11 2 0) Sapphire Substrate[J]. *Applied Physics Letters*, 2020, 117(20): 202102.
- [10] CHAVANNE A, ARNAULT J C, BARJON J, et al. Bias-Enhanced Nucleation of Diamond on Iridium: A Comprehensive Study of the First Stages by Sequential Surface Analysis[J]. *Surface Science*, 2011, 605(5-6): 564-569.
- [11] ICHIKAWA K, KURONE K, KODAMA H, et al. High Crystalline Quality Heteroepitaxial Diamond Using Grid-Patterned Nucleation and Growth on Ir[J]. *Diamond and Related Materials*, 2019, 94: 92-100.
- [12] TRUPINA L, NEDELCU L, BANCIU M G, et al. Texture and Interface Characterization of Iridium Thin Films Grown on MgO Substrates with Different Orientations[J]. *Journal of Materials Science*, 2020, 55(4): 1753-1764.
- [13] KLEIN O, MAYR M, FISCHER M, et al. Propagation and Annihilation of Threading Dislocations during Off-Axis Growth of Heteroepitaxial Diamond Films[J]. *Diamond and Related Materials*, 2016, 65: 53-58.
- [14] LEE K H, SAADA S, ARNAULT J C, et al. Epitaxy of Iridium on SrTiO₃/Si (001): A Promising Scalable Substrate for Diamond Heteroepitaxy[J]. *Diamond and Related Materials*, 2016, 66: 67-76.
- [15] TSUBOTA T, TSURUGA S, SAITO T, et al. Epitaxial Growth of Diamond on an Iridium (100) Substrate by Microwave Plasma-Assisted Chemical Vapor Deposition [J]. *MRS Online Proceedings Library*, 1998, 555(1): 333-338.
- [16] TACHIKI M, FUJISAKI T, TANIYAMA N, et al. Heteroepitaxial Diamond Thin Film Growth on Ir(001)/MgO(001) Substrate by Antenna-Edge Plasma Assisted Chemical Vapor Deposition[J]. *Journal of Crystal Growth*, 2002, 237-239: 1277-1280.
- [17] YAMADA T, YOKOYAMA T, SAWABE A. Electron Emission from Hydrogenated and Oxidized Heteroepitaxial Diamond Doped with Boron[J]. *Diamond and Related Materials*, 2002, 11(3-6): 780-783.
- [18] OHTSUKA K, SUZUKI K, SAWABE A, et al. Epitaxial Growth of Diamond on Iridium[J]. *Japanese Journal of Applied Physics*, 1996, 35(8B): L1072.
- [19] ANDO Y, KUWABARA J, SUZUKI K, et al. Patterned Growth of Heteroepitaxial Diamond[J]. *Diamond and Related Materials*, 2004, 13(11-12): 1975-1979.
- [20] ANDO Y, KAMANO T, SUZUKI K, et al. Epitaxial Lateral Overgrowth of Diamonds on Iridium by Patterned Nucleation and Growth Method[J]. *Japanese Journal of Applied Physics*, 2012, 51(9R): 090101.
- [21] GSELL S, BAUER T, GOLDFÜß J, et al. A Route to Diamond Wafers by Epitaxial Deposition on Silicon via Iridium/Yttria-Stabilized Zirconia Buffer Layers[J]. *Applied Physics Letters*, 2004, 84(22): 4541-4543.
- [22] WU Y, QI J, LEE C H, et al. Diamond Growth on Ir/CaF₂/Si Substrates[J]. *Diamond and Related Materials*, 2003, 12(10-11): 1675-1680.

(下转第 369 页)